An Empirical Model Integrating Dimensional Analysis and Box-Behnken Design for Crack Detection in Rotor Fan Blades

Imran M. Jamadar
Department of Mechanical Engineering, The National Institute of Engineering, [NIE], Mysuru Karnataka India

Ajit Kumar Patil
Department of Mechanical Engineering, The National Institute of Engineering, [NIE], Mysuru Karnataka India

Prasanta Kumar Samal
Department of Mechanical Engineering, The National Institute of Engineering, [NIE], Mysuru Karnataka India

B. Suresha
Department of Mechanical Engineering, The National Institute of Engineering, [NIE], Mysuru Karnataka India

Due to continuous operations and manufacturing errors, fatigue cracks can emerge after hours of service; this causes a fan blade failure and potentially ruins an entire engine, turbo machinery, or rotating machinery of a similar kind. This paper focuses on the condition monitoring of the fan blade for detecting cracks occurring in these blades by analyzing the vibration responses. The mathematical formulation is carried out using the matrix method of dimensional analysis, which is dependent on the fundamental quantities of force, Length, Time, and Temperature (FLTΘ) systems of units. Numerical analysis in ANSYS software is done to comprehend the blade harmonic response for the cracked blade condition. Experimentation is also carried out on Tiera fault simulation machinery equipment, where vibration responses are measured and analyzed for crack detection in the blades. The tests were performed for three different cracks of different lengths and analyzed by varying parameters such as load speed, for which experiments are planned using a Box-Behnken design method. The test results were confirmed with the model equations developed, and notable similarities were seen between the analytical, numerical, and experimental analyses. Thus, the proposed study will help detect the cracks in the blades, thus reducing the serious accidents or failure of the machinery.

Keywords: *Fan Blades, Crack detection, Dimensional analysis, Blade Health Monitoring*

1. INTRODUCTION

Rotating equipment is frequently included in the most important processes in industry, like power generation, aviation, mining, food processing, etc. These industries may have expensive failures due to rotating machinery vibration issues, which can have a detrimental effect on both safety and annual economic losses for businesses. Over time, with the requirement to eliminate expensive company downtime, the attention has shifted considerably towards efficient machinery fault identification and more proactive maintenance methods. Condition-based Mainte–nance (CBM) is a very widespread approach that has attracted a lot of attention in recent couple of decades. Due to errors in manufacturing and fatigue in service cyclic operation, cracks will frequently occur in fan blades.

Vibration measurement provides data both in the time and frequency domain, which will be linked to a fault. However, it is also crucial to evaluate the defect size so as to determine how long blades will still be useful and to prepare for its replacement during routine maintenance. Therefore, it is very important to study the cracked blades' dynamics and explore newer modeling methods.

Kunpeng Xu et al. [1] presented a blade mistuning identification technique for finding blade substrate cracks, which includes crack size and location. Nume–rical and experimental modal analysis was done for the detection of defects. Mengyao Yu et al. [2] proposed a method for recognizing damage to fan blades built on a discrete mathematical model and a fluid-structure analysis. Natural frequencies are acquired for each mode for various locations and sizes of a single crack in a blade. The changes in natural frequencies were an indicator to detect blade damage. A vibration-based approach was discussed to detect cracks in wind turbine blades. In methodology, the operational modal analysis was performed before and after the buckling test by placing the accelerometer along the blade [3]. Sheng Fu and Yinbo Gao [4] put forth a mathematical model and established a correlation between the fan blade's natural frequency and the crack's location and depth.

Modal analysis was also carried out experimentally so as to validate the natural frequency as a fault para–meter. Hwanhee Lee et al. [5] developed a compu–tational model of a rotor-blade system for obtaining the dynamic properties, which showed that the blade pre-twist angle and shaft torsional flexibility have a notable effect on the system's varying response. Neri and Peeters [6] presented a harmonic Fourier analysis appr–oach for detecting blade cracks quantitatively. A data processing algorithm was established to obtain the fre–quency shift from short-time samples. Rama Rao and Dutta [7] analyzed the compressor blade's failure in a gas turbine. Ultrasonic technique and vibration measu–rement were effectively implemented to investigate the root cause of

Received: May 2023, Accepted: November 2023
Correspondence to: Dr Imran M Jamadar, Department of Mechanical Engineering, The National Institute of Engineering, [NIE], Mysuru, Karnataka, India.
Email: imranjamadar2@gmail.com
doi: 10.5937/fme2401045J

the blade failure. J. Xie et al. [8] presented a blade health moni–toring method based on the statistical index of the shaft's random vibration in the frequency domain. A blade disc shaft coupled model was developed, and monitoring indices such as mean frequency and bandwidth were ef–fectively used for damage identification. Xie J S et al. [9] proposed a theoretical model for a rotating blade having a breathing crack. The coupling of the centrifugal force, breathing effects, and crack effect was made in the model. H. Guo et al. [10] presented a tip timing method based on synchronous resonance vibration measurement for blade damage detection. The method was verified with the experimental results, and it concluded that the identification of the blade resonance parameter without a once-per-revolution (OPR) sensor was achieved. Guru, S. S. et al. [11] explored the use of the blade tip timing (BTT) method for preventative forecasting of rotor blade damage. The method measures blade natural frequencies in combination with blade tip position during engine testing. A fusion of eddy current and optical sensors, which were located circumferentially on the aero engine's casing, was used to attain the resonance order for the bending mode vibration of the blade. Nelson and Nataraj [12] developed an analytical procedure for the simulation of dynamic characteristics of rotor bearing assembly ha–ving a crack of transverse by FEM representation and perturbation parameter to understand the local stiffness changes caused due to the crack. Ming Chuan Wu and Shyh-Chin Huang [13], using the technique of released energy, examined the dynamic characteristics of a rota–ting blade with a transverse crack. Displacement respon–ses of the blades having cracks were discussed under uniform lateral forces. Joshuva and Sugumaran [14] reported fifteen tree classification-based machine learning methods in order to locate and detect wind turbine blade cracks. These models were developed by computing the blade's vibration response obtained with a piezoelectric accelerometer.

Jun Lin et al. [15] implemented a novel BTT analysis method that acquires the vibrating blade tip's arrival time when the blades pass through a BTT probe and reconstructs two or more modes of blade vibration signals. Krause and Ostermann [16] used an Acoustic Emission (AE) approach to find damage to wind turbine rotor blades via airborne sound; with a close match to the recorded damage occurrences, the real-time opera–ting algorithm determines the significance of the iden–tified damages. Ken and Martin [17] developed app–roaches for measuring torsional natural frequencies to a jet engine that had experienced disc breaking near the blade root, as well as blade cracking by the resampling method. Xu Jinghui et al. [18] reported a method based on the synchro-extracting transform having the advan–tage of high time frequency through the natural frequency shift for the damage detection of rotor blades. Ogbonnaya, E.A. et al. [19] studied the dynamic res–ponse of marine gas turbine rotor shaft systems exposed to force harmonic excitation. F. L. M. dos Santos et al. [20] used modal strain energy and coordinate modal assurance criterion (COMAC) to detect an entire-size composite helicopter rotor blade damage. In these methods, the detection is based on comparing vibration modes and modal strain energy of the beam. Z. Fan et al. [21] focused on the parameter identification techni–que of blade vibration measurements. The method was discussed both using theoretical and experimental analysis. Blade strain measurement was used to verify the parameter identification method's accuracy, and the results were compared with other BTT methods. Wens–heng Zhao et al. [22] investigated the failure of a low-pressure steam turbine in a pressurized water reactor (PWR) power plant and analyzed the dynamical charac–teristics both experimentally and numerically. Wang et al. [23] used the difference in mode shape curvature for fault detection and finite element method (FEM) for dynamic behavior (modal analysis and response ana–lysis). Alterations in natural frequencies and modes for the small-size blades with faults were seen to occur at lower frequencies than that of larger-size blades. A. Sarrafi et al. [24] proposed a phase-based motion esti–mation (PME) and motion magnification algorithm for damage detection in the wind turbine blades; a sequence of images was extracted by PME and investigated for the damage detection, deflection in shapes during the operations of the blades and was compared for the baseline with the damaged state which helped in detec–ting the damage in the blades. T. Zhang et al., [25] presented a fusion of vibroacoustic signal and one-di–mensional convolution neural network for damage detection in centrifugal fan blades. Marjan Djidrov et al. [26] presented a vibration frequency response analysis for beam damage detection. Numerical analysis was performed for cantilever beam configuration using ANSYS. O. I. Abdullah et al. [27] studied wind turbine blades for deformations and stresses under steady-state loading and investigated the vibration characteristics such as natural frequency and mode shapes by finite element analysis.

An overview of the literature on identifying and assessing blade vibration and health issues in rotating machinery is provided. This section briefly explains condition monitoring approaches, vibration-based fault diagnosis, and different vibration measurement techni–ques that are typically used to find the blade's health conditions in rotating machines. In this work, the blade crack detection analysis is made through vibration ana–lysis; the frequency response of the bladed disc-rotor system by varying different parameters such as load, speed, and defect conditions is obtained numerically and experimentally. Also, a mathematical model is estab–lished using matrix dimensional analysis, which has yet to be attempted and seen from the literature review for the fan blade crack detection so far for obtaining the frequency response from cracked blades. Moreover, most studies on the damage detection of blades are related to testing it in stationary conditions wherein the changes in mode shapes and natural frequencies were witnessed for possible causes of the defect. But the fan blade, being a continuously rotating member, needs methodologies for monitoring it in running condition. The proposed method here focuses mainly on the running condition testing of fan blades in

that examining the cracked blades' frequency response is the key point to implementing this method.

2. MATHEMATICAL MODELING

Dimensional analysis has classically been used to solve problems related to fluid mechanics or heat exchange problems up to this. But, because of its ability and simplicity in simulating complex issues, it has drawn the interest of numerous researchers and has recently been used in the condition monitoring of turbomac–hinery industries. Using dimensional analysis, the cont–rollable and uncontrollable variables in an experimental investigation can be easily separated and placed in a non-dimensional manner [28]. Thereby reducing the variables and experiments to a minimum. The variables that affect the dynamic behavior of the rotor blade system are given in Equation 1.

$$R = f(r_2, r_1, r_{ws}, L_s, t_d, E, \rho, L_b, w_b, t_b, \Delta, N, W) \quad (1)$$

Here 'R' is a response parameter linked to the fre–quency response of the rotor blade shaft system for varying factors such as load, speed, and defect size (fundamental variables). The frequency response of the defective system is dependent on different designs and operating variables, as given in Table 1 in the FLTΘ system of units.

Table 1: Parameters and Dimensions of the Bladed Disk Rotor

Parameters	Dimensions
External diameter of disk (r_2)	L
Internal diameter of disk (r_1)	L
Radius of shaft (r_s)	L
Length of shaft (L_s)	L
Thickness of disk (t_d)	L
Young's modulus (E)	$F^1 L^{-2}$
Poisson ratio (μ)	---
Density of blade (ρ)	$F^1 L^{-4} T^2$
Blade Length (L_b)	L
Blade Width (w_b)	L

In matrix form, these fundamental factor is repre–sented in Table 2.

Table 2 Matrix of the repeated factors

Dimension	R_1	R_2	R_3
F	R_{11}	R_{12}	R_{13}
L	R_{21}	R_{22}	R_{23}
T	R_{31}	R_{32}	R_{33}

Non-repeating variables from Equation (1), which also includes frequency response, the matrix is provided in Table 3. The matrix in Table 3 is of the order (3xn), where 'n' is the number of variables remaining known as un-repeated variables.

According to the matrix method, any n^{th} dimensionless group can be formulated as,

$$\frac{U_n}{R_1^{C1n} R_2^{C2n} R_3^{C3n}} = F^0 L^0 T^0 = (\pi_n) \quad (2)$$

Table 3 Dimensional matrix for Un-repeated variables

Dimension	U_1	U_2	U_3	……	U_n
F	U_{11}	U_{12}	U_{13}	…….	U_{1n}
L	U_{21}	U_{22}	U_{23}	…….	U_{2n}
T	U_{31}	U_{32}	U_{33}	…….	U_{3n}

A non-dimensional group always equals the number of non-repeating variables (n) involved. In this case, n = 11, using the matrix method, these dimen–sionless variables are obtained. Once we substitute the variable from Tables 2 and 3 in above Eq. (2), we get,

$$\frac{\left(F^{U1n} L^{U2n} T^{U3n}\right)}{\left(F^{U11} L^{U21} T^{U31}\right)^{C1n} \left(F^{U21} L^{U22} T^{U32}\right)^{C2n} \left(F^{U13} L^{U23} T^{U33}\right)^{C3n}} = (\pi_n) \quad (3)$$

where C_{1n}, C_{2n}, and C_{3n} are the unknown parameters. These are derived by formulating the linear system of equations as,

$$\begin{aligned} R_{11}C_{1n} + R_{12}C_{2n} + R_{13}C_{3n} &= U_{1n} \\ R_{21}C_{1n} + R_{22}C_{2n} + R_{23}C_{3n} &= U_{2n} \\ R_{31}C_{1n} + R_{32}C_{2n} + R_{33}C_{3n} &= U_{3n} \end{aligned} \quad (4)$$

The above set of equations can be represented in the matrix form as,

$$\begin{bmatrix} R_{11} & R_{12} & R_{13} \\ R_{21} & R_{22} & R_{23} \\ R_{31} & R_{32} & R_{33} \end{bmatrix} \begin{Bmatrix} C_{1n} \\ C_{2n} \\ C_{3n} \end{Bmatrix} = \begin{Bmatrix} U_{1n} \\ U_{2n} \\ U_{3n} \end{Bmatrix} \quad (5)$$

Further, it is simplified as,

$$[R][C] = [U] \quad (6)$$

By doing an inversion of the matrix, the unknowns in Equation (5) are found, which are listed in Table 4.

$$[C] = [R]^{-1}[U] \quad (7)$$

Hence, Equation (1) in non-dimensional form is represented by,

$$\Pi_R = f(\Pi_1, \Pi_2, \Pi_3, \Pi_4, \Pi_5, \Pi_6, \Pi_7, \Pi_8, \Pi_9, \Pi_{10}) \quad (8)$$

It requires that,

$$f(\Pi_1, \Pi_2, \Pi_3, \Pi_4, \Pi_5, \Pi_6, \Pi_7, \Pi_8, \Pi_9, \Pi_{10}) = 0 \quad (9)$$

After substituting all the dimensionless relations, we get,

$$\Pi_R = f\left[\frac{L_b}{\Delta} \; \frac{W_b}{\Delta} \; \frac{t_b}{\Delta} \; \frac{\rho\Delta^4 N^2}{W^1} \; \frac{E\Delta^2}{W^1} \; \frac{t_d}{\Delta} \; \frac{r_1}{\Delta} \; \frac{r_2}{\Delta} \; \frac{r_2}{\Delta} \; \frac{L_s}{\Delta}\right] \quad (10)$$

Table 5 Shortened Dimensionless Variables

$\Pi_{simplified}$	
$\Pi_a = \frac{\Pi_7}{(\Pi_1 \times \Pi_3)}$	$\Pi_b = \Pi_9$
$\Pi_c = \frac{(\Pi_2 \times \Pi_5 \times \Pi_8)}{\Pi_4}$	$\Pi_d = \frac{1}{(\Pi_6 \times \Pi_{10})}$

The number of dimensionless groups is still more; they are reduced further by simplifying as given in Table 5 [29].

Hence, equation (10) in simplified form is,

$$\Pi_R = f\left(\Pi_a \times \Pi_b \times \Pi_c \times \Pi_d\right)$$

$$\Pi_R = \frac{f_{br}}{f_S} = \left(\frac{\Delta^* r_1}{t_b * L_b} \quad \frac{r_s}{\Delta} \quad \frac{EW_b r_2}{\Delta^4 N^2 \rho} \quad \frac{\Delta^2}{t_d L_S} \right) \tag{11}$$

Now, to assess the defects from the obtained frequency responses from defective blade components, Equation (11) is written in power law form.

$$\Pi_R = \phi \times \left(\frac{\Delta^* r_1}{t_b * L_b} \right)^{a1} \times \left(\frac{r_s}{\Delta} \right)^{a2} \times \left(\frac{W_b E r_2}{\Delta^4 N^2 \rho} \right)^{a3} \times \left(\frac{\Delta^2}{t_d L_S} \right)^{a4} \tag{12}$$

Equation (12) represents the mathematical model for assessing frequency response from the defects in blades. In Equation (12), ϕ, a_1, a_2, a_3, a_4 are the unknowns. These are achieved by doing multiple factorial regression by **means** of the least square method [30]. To obtain the unknowns, taking logarithms on both sides of Equation (12) and letting,

$$\log\left(\frac{f_{br}}{f}\right) = y \qquad \log(\varphi) = a_0 \qquad \log\left(\frac{\Delta^* r_1}{t_b * L_b}\right) = x_1$$

$$\log\left(\frac{r_s}{\Delta}\right) = x_2 \quad \log\left(\frac{W_b E r_2}{\Delta^4 N^2 \rho}\right) = x_3 \quad \log\left(\frac{\Delta^2}{t_d * L_s}\right) = x_4$$

Hence, Equation (12) becomes,

$$y = a_0 + a_1 x_1 + a_2 x_2 + a_3 x_3 + a_4 x_4 \tag{13}$$

If 'n' experiments are to be piloted to obtain unknowns, then the results obtained will be grouped up using Equation (14).

$$\sum_{i=1}^{n} y_i = n a_0 + a_1 \sum_{i=1}^{n} x_{i1} + a_2 \sum_{i=1}^{n} x_{i2} + a_3 \sum_{i=1}^{n} x_{i3} + a_4 \sum_{i=1}^{n} x_{i4} \tag{14}$$

Five equations must be created so as to evaluate five unknowns. The other equations are derived by separately multiplying x_{i1}, x_{i2}, x_{i3} and x_{i4} with Equation (14) and written in matrix form given in Equation (15).

$$\begin{bmatrix} n & \sum x_{i1} & \sum x_{i2} & \sum x_{i3} & \sum x_{i4} \\ \sum x_{i1} & \sum x_{i1}x_{i1} & \sum x_{i1}x_{i2} & \sum x_{i1}x_{i3} & \sum x_{i1}x_{i4} \\ \sum x_{i2} & \sum x_{i2}x_{i1} & \sum x_{i2}x_{i2} & \sum x_{i2}x_{i3} & \sum x_{i2}x_{i4} \\ \sum x_{i3} & \sum x_{i3}x_{i1} & \sum x_{i3}x_{i2} & \sum x_{i3}x_{i3} & \sum x_{i3}x_{i4} \\ \sum x_{i4} & \sum x_{i4}x_{i1} & \sum x_{i4}x_{i2} & \sum x_{i4}x_{i3} & \sum x_{i4}x_{i4} \end{bmatrix} \begin{bmatrix} a_0 \\ a_1 \\ a_2 \\ a_3 \\ a_4 \end{bmatrix} = \begin{bmatrix} \sum y_i \\ \sum x_{i1}y_i \\ \sum x_{i2}y_i \\ \sum x_{i3}y_i \\ \sum x_{i4}y_i \end{bmatrix} \tag{15}$$

Table 4. Unknowns for formulating dimensionless groups

	r_1	r_2	W	E	ρ	w_b	Δ	r_S	t_b	N	Ls
C_{1n}	1	1	0	-2	-4	1	1	1	1	0	1
C_{2n}	0	0	0	0	-2	0	0	0	0	-1	0
C_{3n}	0	0	1	1	1	0	0	0	0	0	0

A code is written to get unknowns in Equation (15) by solving the matrix inversion in Matlab software using the experimental data set.

3. DESIGN OF EXPERIMENTS

Design of experimentation (DOE) is a sequence of statistics used to conduct the fewest number of experiments. These are needed to get the greatest amount of relevant information about the variables/factors impacting the response of the process/ phenomenon.

By considering the consequence of various factors on the system's response, statistical analysis has to be done by setting the factors at the desired level. Fisher invented one of the important types of DOE called a factorial region. This factorial region is the one in which one factor is set to a mid-level, and the groupings of the other two factors are applied. The key benefit of this is that it reduces the total number of experiments to be performed when matched with the full factorial region experiments [31].

3.1 Box Behnken Design (BBD)

The Box–Behnken design (BBD) was invented by Box and Behnken in 1960 to have an appropriate response surface of a three-factorial design. Box-Behnken De–signs are utilized to enhance experiment design for varying factors. According to BBD, 3 factors involve three blocks, in each of which 2 factors are varied thro–ugh the 4 possible combinations of high and low. It is necessary to include center points as well (in which all factors are at their central values), as shown below in Figure 1 [32].

Table 6. DOE's Combinations from Box-Behnken Design

Expt.	Speed (rpm)	Load (Kg)	Defect Size (mm)
1	1000	1	9
2	2000	0	9
3	1000	1	3
4	2000	2	3
5	3000	1	3
6	3000	1	9
7	1000	0	6
8	2000	0	3
9	3000	2	6
10	2000	1	6
11	2000	2	9
12	1000	2	6
13	2000	1	6
14	3000	0	6
15	2000	1	6

The learning of the impact of various variables on the results of a controlled experiment is the core of the DOE toolset [32]. The designs that are obtained are very suitable for conducting the trials of experiments, and they are also rotatable. In our study, three factors, i.e., Δ, W, and N, each with three levels, have been chosen to execute the BBD by using a MINITAB software package for having a vibration frequency response due to varying factors such as defect size, speed, and load. There are 15 combinations of these factors, as given in Table 6, for verification of the dependency of these factors on the vibration frequency response.

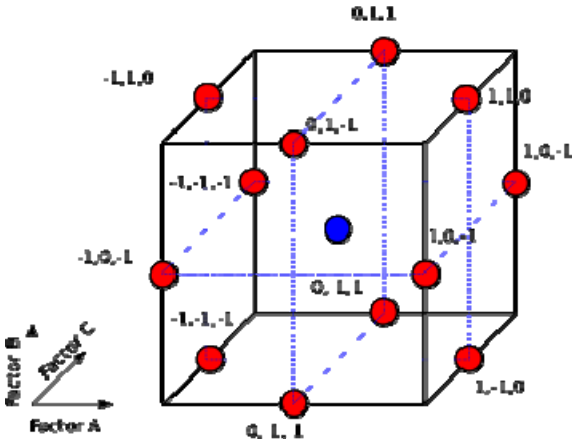

Figure 1. Box–Behnken design

3.2 Finite Element Analysis (FEA)

Performing the finite element analysis as a reference, the cracked blade model is investigated and compared in this study. Geometric modeling is worked out in Solidworks software, where detailed design dimensions of the system are given in Table 7. Figure 2 (a) shows the blades model developed in solid-works software. Here, the blades of defects having a crack length of 3 mm, 6 mm, and 9 mm are created. The complete assembly of the blades-shaft-disc rotor system for varying loads is given in Figures 2 (b)-(d), respectively.

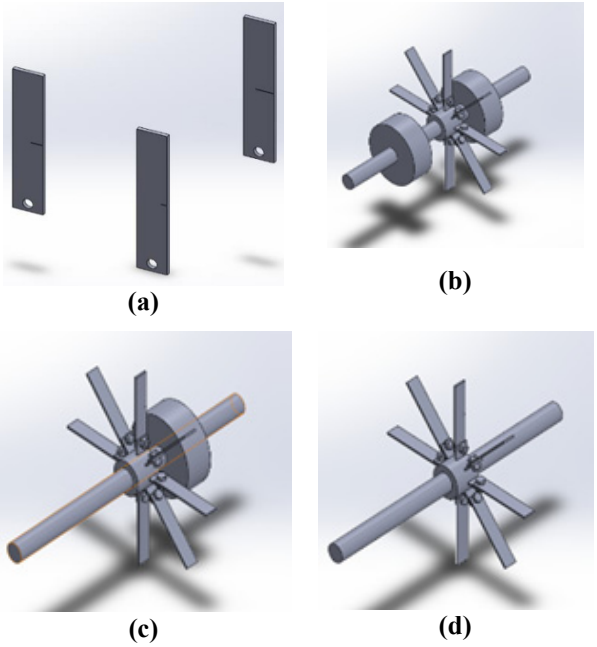

(a) (b) (c) (d)

Figure 2. (a) Defective fan blades (b) Rotor with two loads (c) Rotor with one load (d) Rotor with no load

The design model of a blade disk shaft system is imported from the SOLIDWORKS Software to ANSYS Workbench, and the material properties of the system and mesh of the geometry are also carried out by selecting the suitable element size. A typical modeling mesh for the shaft-disc-blades system is illustrated for a 2 mm element size. The convergence study exhibited that the element number and size are appropriate for the convergence of the results. Modal structural analysis in ANSYS Workbench software is done to explore the behavior of the blade-shaft-disc system for the desig–nated boundary conditions for different DOEs. Harmo–nic analysis is performed to understand how a structure will respond to sinusoidal repeating dynamic loading; the boundary conditions were allocated to the blade-shaft-disc system by understanding the bearings' loca–tion, depicted in Figure 3. Depending on the real-time support conditions, the shaft is assigned with the boun–dary condition available in ANSYS, with no movements in the (X, Y) directions. So, the translation and rotation in the X and Y directions are constrained, and in the Z direction, the constraint is only for transitional, and for rotation, it is set to be free. Similar boundary conditions were consigned for all the DOEs listed in Table 6.

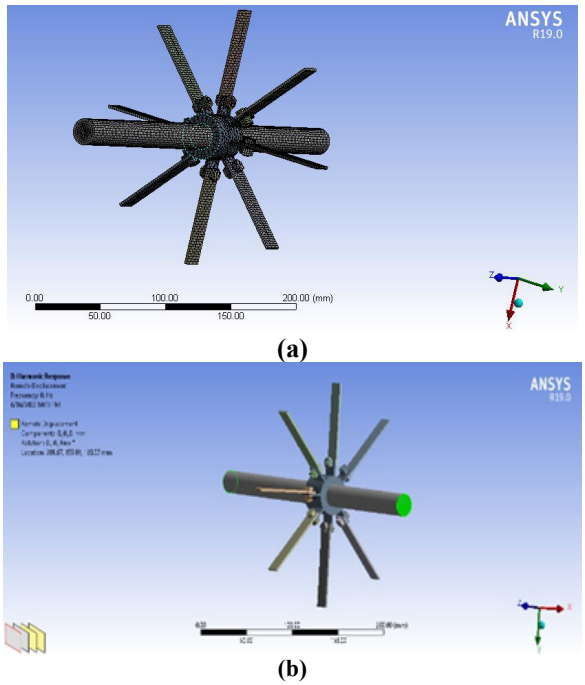

(a) (b)

Figure 3. (a) Meshing (b) Boundary conditions

Table 7 Model Parameters of the System

Symbols	Values
Length of blade (L)	75 mm
Width of blade (w_b)	15 mm
Thickness of blade (t_b)	2 mm
Thickness of disk (t_d)	35 mm
External radius of disk (r_2)	17.5 mm
Internal radius of disk (r_1)	10 mm
Radius of shaft (r_s)	20 mm
Shaft length (S)	320 mm

The first harmonic of the frequency for each design configuration from DOE's is noted. The simulation is carried out for three defect size conditions having crack lengths of 3 mm, 6 mm, and 9 mm, respectively, having two load discs of mass 1 kg each. The speed is altered from 1000 rpm 2000 rpm, and to 3000 rpm. The noted first harmonic frequency for all the Design of Experiments (DOE's) is recorded in Table 8, and res–ponses for some of the trials are provided in Figure 4.

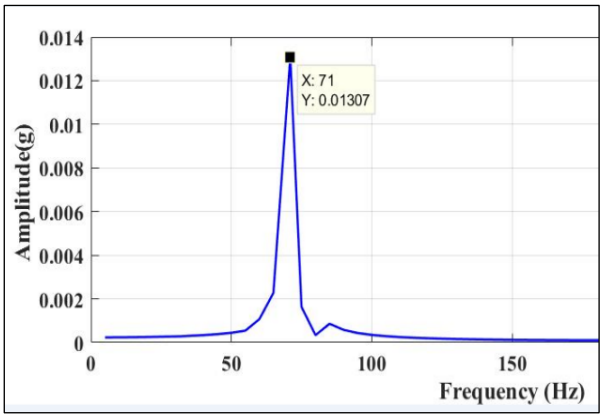

(a) Simulation 2

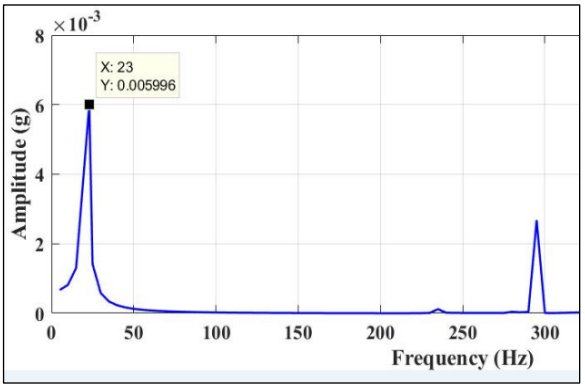

(b) Simulation 4

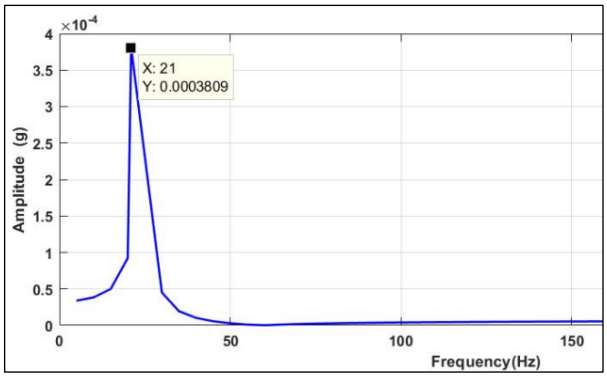

(c) Simulation 5

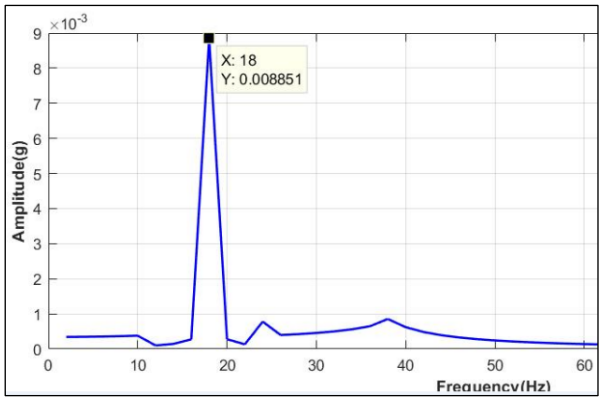

(d) Simulation 10

Also, during the higher speed trails, the centrifugal forces cause tensile stress in the cracked surface, and as the crack is open all the time during rotation, the non-linear response characteristic is extinct from the spectrum shown in Fig.4.

3.3 Experimental Analysis

In this study, the experimentation is performed on equipment called Tiera fault simulation machinery to diagnose the crack in the blades and the vibration response of the blade when it is exposed to load, change in speed, and defect sizes. The blades with artificially induced cracks of three different lengths and fabricated blade assemblies are depicted in Figure 5.

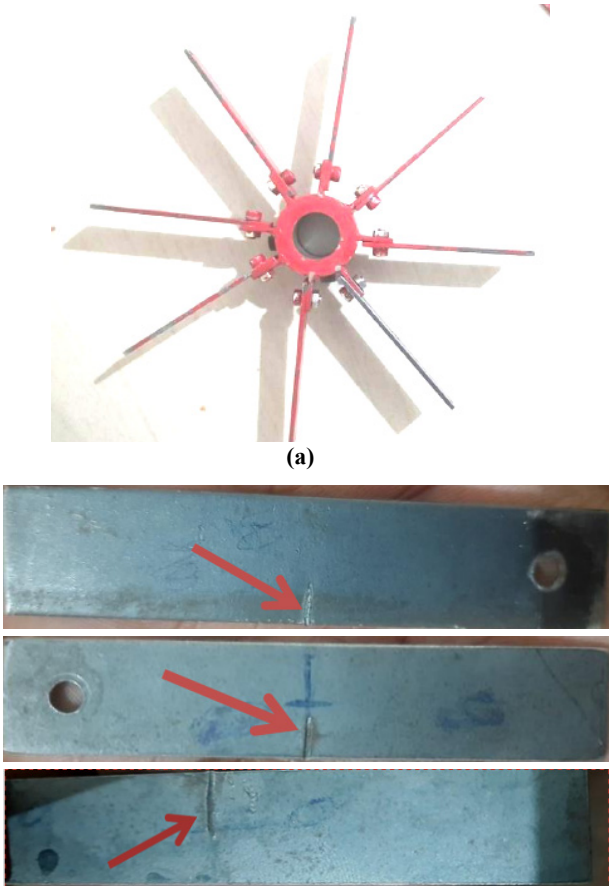

(a)

(b)

Figure 5 (a) Fabricated blade assembly (b) Defective blades of different crack lengths

The experimental test rig is depicted in Figure 6. The test rig setup mainly comprises a driver 3-phase squirrel cage induction motor, 2 bearing pedestals, and bearing adapters. A shaft made of steel has a 600 mm length and diameter of 20 mm, where one or more bladed discs can be inserted. A variable speed controller increases and decreases the speed which is connected to a motor. A flexible coupling between a motor shaft and rig rotor and a rugged carrying case to cover safety precautions. The defective blades are replaced according to the DoE conditions, the load is varied, and the blade is made to run at the required speed. Once the machine is running for a particular condition, the output is obtained using a Software called TIERA (Data Acquisition System, Make: TIERA, Model: T-DAQ IEPE -2605, SL No: IEPE-0022-0225-0055).

The data acquisition uses the accelerometer Sensor 2 Nos, Make: CTC, Model: MEB210, SL Nos: 2696, 2701 placed at the drive and non-drive end.

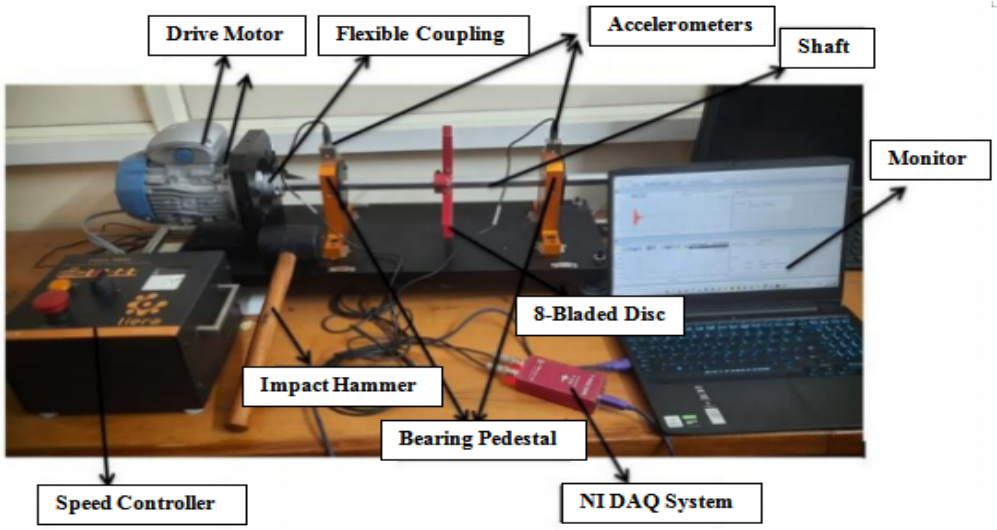

Figure 6. Experimental setup and data acquisition system

4. RESULTS AND DISCUSSIONS

Experiments are performed as per the design matrix provided in Table 6, and the first harmonic frequency response of the system for different conditions is obtained. Each experiment is repeated two times so as to ensure the repeatability of the results. In which setting has been given for collecting the frequency and time domain data [33,34]. Once the output is obtained using the software, the data is obtained, and the graphs are plotted in the LABVIEW software. The outcomes of finite element simulation and experiments are provided in Table 8. Figure 7 shows the harmonic frequency response for different trials obtained using the Design of Experiments (DOEs) enlisted in Table 8.

As seen in Figure 6, the first harmonic response of the frequency is the dominant one, clearly indicating the presence of the fault. The additional bending moment because of centrifugal forces increased, and the asymmetry of the peaks in the vibration spectrum increased, as seen in Figure 6. ANOVA using MINITAB is carried out for the experimental data obtained, and the data is listed in Table 9, having a predictive accuracy of 99.78%. The results obtained from the experimentation are very close to simulation results in ANSYS and are acceptable. The contribution or the effect of the parameters on the frequency response is also given in Table 8; the most affecting parameter to the frequency response is defect size, with a contribution of 59.75 %. Load and speed affect 11.20% and 0.029%, respectively.

Table 8. Comparison of Frequency response by FEM and experimentation

Expt.	Speed (rpm)	Load (Kg)	Defect Size (mm)	Frequency Response By FEM (Hz)	Frequency Response By Experiments (Hz)
1	1000	1	9	51	50
2	2000	0	9	71	70
3	1000	1	3	22	21
4	2000	2	3	23	22
5	3000	1	3	21	24
6	3000	1	9	50	51
7	1000	0	6	33	32
8	2000	0	3	32	31
9	3000	2	6	18	19
10	2000	1	6	25	24
11	2000	2	9	49	50
12	1000	2	6	19	18
13	2000	1	6	25	24
14	3000	0	6	32	34
15	2000	1	6	25	24

Table 9. ANOVA- Experimental results

Parameter	DF	SS	MS	F	Contribution
Regression	9	3366.48	374.05	257.97	99.78
Linear	3	2394.25	798.08	535.23	70.96
Defect size	1	2016.13	2016.13	1390.4	59.75
Speed	1	1	1	1	0.02964
Load	1	378.13	378.13	260.78	11.20
Square	3	939.98	313.33	216.09	27.86

Interaction	3	32.25	10.75	7.41	0.9559
R. Error	5	7.25	1.45		
Lack of Fit	3	7.25	2.42		
Pure Error	2	0.000000	0.000000		
Total	14	3373.73			
R^2= 99.78% % R^2(Adj.)= 99.18%					

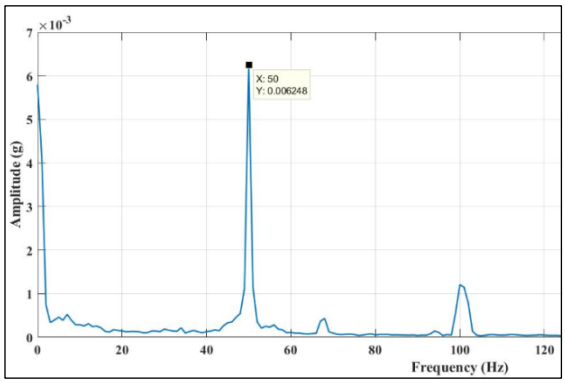

(a)

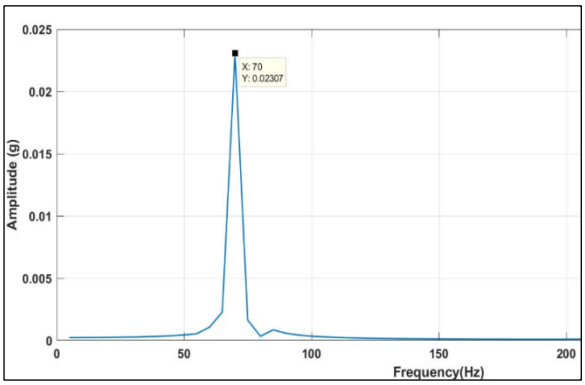

(b)

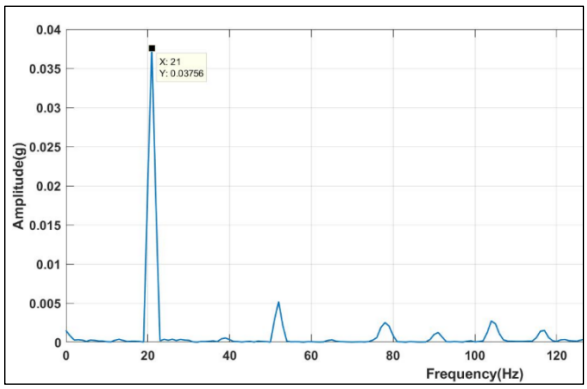

(c)

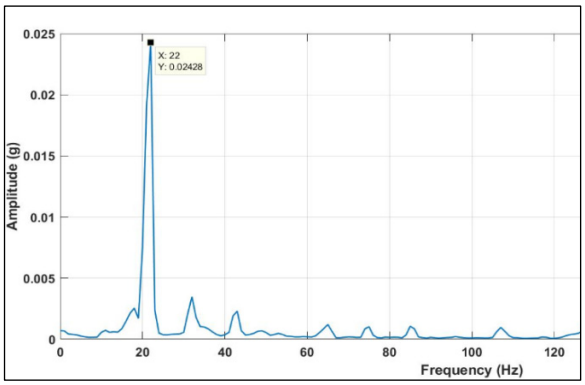

(d)

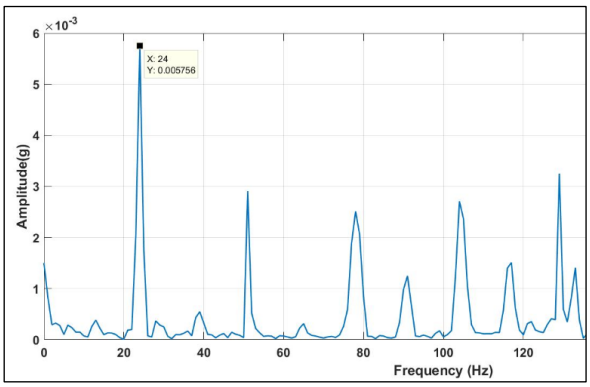

(e)

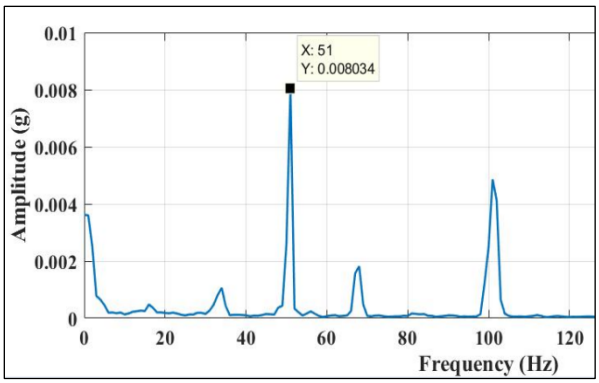

(f)

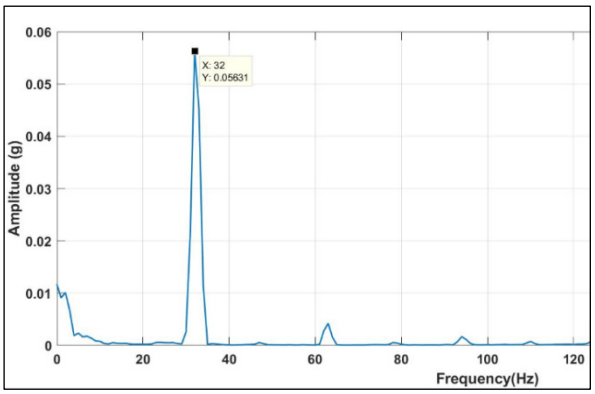

(g)

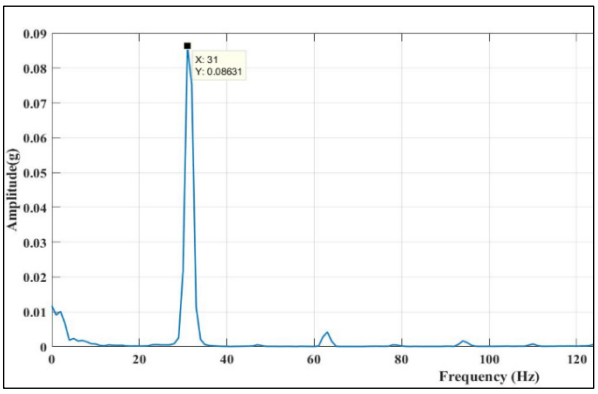

(h)

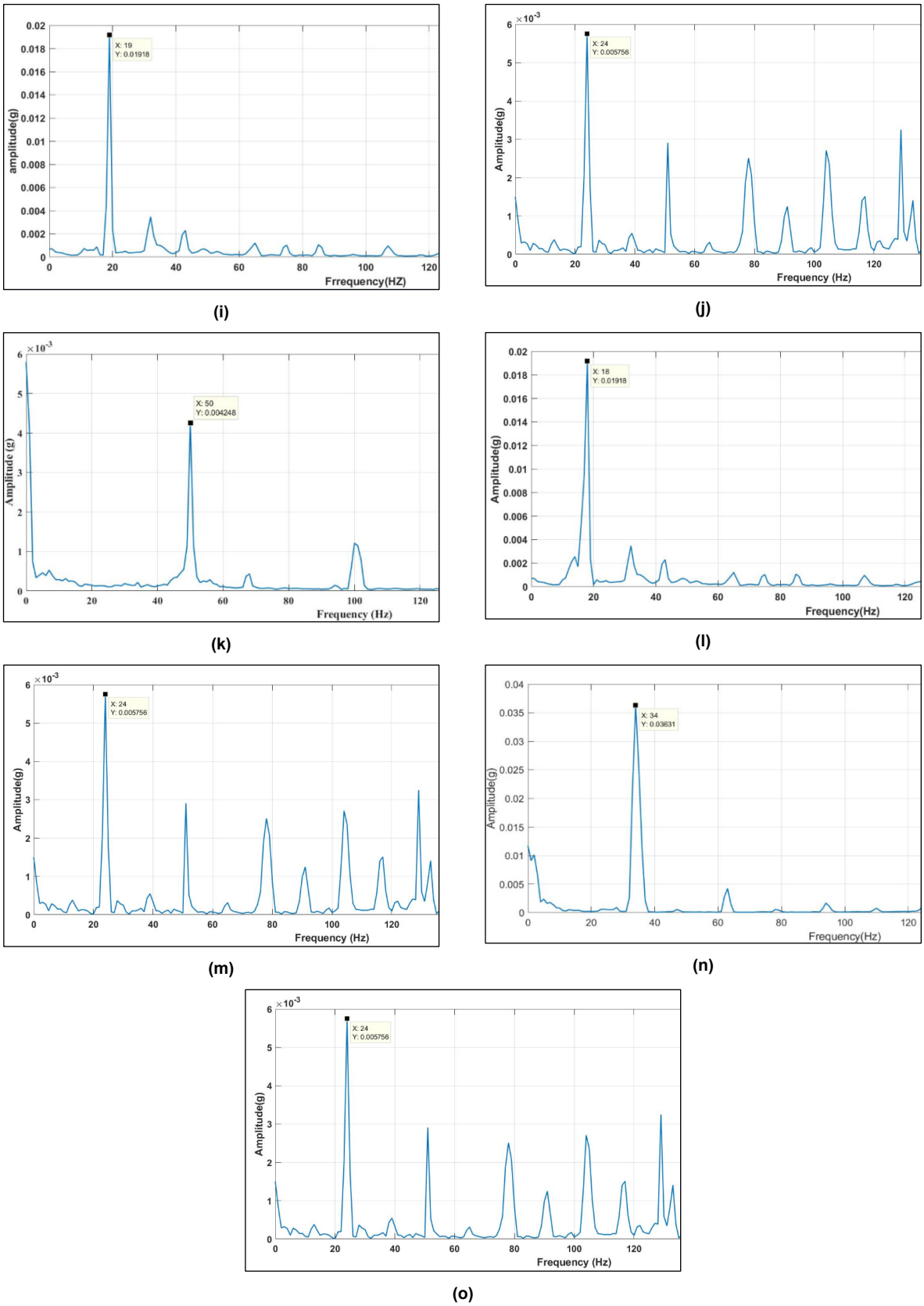

Figure 7. Experimental Frequency Spectrum for DoE's

Table 10. Comparison of Frequency response by Model Equation and experimentation

Expt.	Speed (rpm)	Load (Kg)	Defect Size (mm)	Frequency Response By Experiments (Hz)	Coded Response (Dimensionless)	Response from Equation (12) (Dimensionless)
1	1000	1	9	50	3	2.73
2	2000	0	9	70	2.1	2.02
3	1000	1	3	21	1.26	1.14

4	2000	2	3	22	0.66	0.59
5	3000	1	3	24	0.4	0.4
6	3000	1	9	51	1.02	0.92
7	1000	0	6	32	1.92	1.83
8	2000	0	3	31	0.93	0.83
9	3000	2	6	19	0.38	0.34
10	2000	1	6	24	0.72	0.63
11	2000	2	9	50	1.5	1.43
12	1000	2	6	18	1.08	1.03
13	2000	1	6	24	0.72	0.74
14	3000	0	6	34	0.68	0.64
15	2000	1	6	24	0.72	0.69

Speed has an almost negligible effect on the first harmonic response frequency of the system. Varying the load with blade defects will certainly vary the first harmonic response frequency. As per the mathematical Equation (12) developed in section 2, and using the first harmonic response frequency data obtained from the experimentation, mathematical calculations were formed using the Equation (15), and the coded freque–ncy response, i.e. $(\frac{f_{br}}{(f_s)})$ obtained using the equations are provided in Table 10. The suggested empirical model can provide almost similar accuracy to FEA's by making comparative analyses at different speeds and load values. Initially, the response frequency obtained will be Hz. To make it dimensionless, we multiply the response frequency by the shaft speed at which the response frequency is obtained to get the coded response, as presented in Table 9. The values of a_1, a_2, a_3, a_4, and a_5 obtained on solving equation 15 from section 2 are -1.174, 6.0237, 1.4219, 0.4768, -1.0088. Using the mathematical Equation (12), the predicted frequency responses for all 15 combinations of DOEs almost match the frequency response obtained during experimentation. A small deviation is considerable because of the mistuned effect that might be attributed to blade fabrication and fitting.

5 CONCLUSIONS

Local flexibility is caused by cracks in the blades, which occur due to manufacturing errors and fatigue due to high cycle (HCF). Consequently, safe and robust blade vibration recording and fault alerting play a vital role in rotating machinery health management. In this study, Numerical and experimental analyses were per–formed on a test rig having a rotor with an 8-bladed disc by varying parameters such as load, speed, and blade crack size. Design of experiments (DOEs) are obtained using the Box-Behnken method for executing the experimental analysis. The conclusions obtained from the work undertaken are given below.

- The defect size/crack length contribution in the frequency response variation is more when com–pared to the other parameters like load and speed, which is 59.75 %. The predictive accuracy obtai–ned for this using ANOVA is 99.78% and is above 95%, indicating the results obtained to determine faults in fan blades are validated.
- The mathematical equations developed using the dimensional analysis predicted response frequency almost equal to the data obtained in experimental analysis, where there is a small deviation due to some common experimental errors.
- This work helps in understanding the cracks occurring in the blades through the frequency responses analysis; because of the breathing effect of the crack, the harmonics up to 2x of the rotor spin frequency appear in the vibration spectrum.
- As crack length increases, there will be a variation in the harmonic frequency when it is compared with the shaft-disc-blades having undamaged blades.
- During the higher speed trails, the centrifugal for–ces cause tensile stress in the cracked surface, and as the crack is open all the time during rotation, the non-linear response characteristic is extinct from the spectrums.

REFERENCES

[1] Kunpeng, X. et al.: Detection of blade substrate crack parameters of hard-coated blisk based on mistuning identification technology, Mechanical Systems and Signal Processing, Vol. 165, 108381, 2022.

[2] Mengyao, Y., Sheng, F., Yinbo, G., Hao, Z., and Yonggang, X.: Crack Detection of Fan Blade Based on Natural Frequencies, International Journal of Rotating Machinery, Vol. 2018, Article ID 2095385, 13 pages, 2018.

[3] Lorenzo, ED., Petrone, G., Manzato, S., Peeters, B., Desmet, W., and Marulo, F.: Damage detection in wind turbine blades by using operational modal analysis. Structural Health Monitoring, Vol.15(3), pp.289-301, 2016.

[4] Fu, S., and Gao, Y.: Fan blade crack diagnosis method study, Advances in Mechanical Engineering, Vol.8(5), pp.1-8, 2016.

[5] Lee, H., Song, JS. and Cha, SJ.: Dynamic response of coupled shaft torsion and blade bending in rotor blade system. Journal of Mechanical Science and Technology, Vol.27, pp.2585–2597, 2013.

[6] Neri, P., and Peeters, B.: Non-Harmonic Fourier Analysis for bladed wheels damage detection, Journal of Sound and Vibration, Vol. 356, pp.181-194, 2015.

[7] Rama Rao, A., and Dutta, B.K.: Vibration analysis for detecting failure of compressor blade, Engine–ering Failure Analysis, Vol. 25, pp. 211-218, 2012.

[8] Jingsong, X., Jie, L., Jinglong, C., and Yanyang, Z.: Blade damage monitoring method base on frequency domain statistical index of shaft's random vibration, Mechanical Systems and Signal Processing, Vol. 165, 108351, pp.1-21, 2022.

[9] Xie, J., Zi, Y., and Zhang, M.: A novel vibration modeling method for a rotating blade with breathing cracks, Science China, Technological Sciences, Vol. 62, pp.333–348, 2019.

[10] Haotian, G., Fajie, D., and Jilong, Z.: Blade resonance parameter identification based on tip-timing method without the once-per revolution sensor, Mechanical Systems and Signal Processing, Vol. 66–67, pp.625-639, 2016.

[11] Guru, S., Shylaja, S., Kumar, S., and Murthy, R.: Pre-emptive Rotor Blade Damage Identification by Blade Tip Timing Method, ASME Journal of Engineering for Gas Turbines Power, Vol.136 (7): 072503, pp.1-4, 2014.

[12] Nelson, H. D., and Nataraj, C.: The Dynamics of a Rotor System with a Cracked Shaft, ASME Journal of Vibration, Acoustics, Stress, and Reliability, Vol.108 (2), pp.189–196, 1986.

[13] Ming-Chuan, W., and Shyh-Chin, H.: On the vibration of a cracked rotating blade, Shock and Vibration, Vol. 5, pp.317–323, 1998.

[14] Joshuva, A., and Sugumaran, V.: Crack Detection and Localization on Wind Turbine Blade Using Machine Learning Algorithms: A Data Mining Approach, Structural Durability & Health Monitoring, Vol.13(2), pp.181–203, 2019.

[15] Jun, L., Zheng, H., Zhong-Sheng, C., Yong-Min, Y., and Hai-Long, X.: Sparse reconstruction of blade tip-timing signals for multi-mode blade vibration monitoring, Mechanical Systems and Signal Processing, Vol. 81, pp. 250-258, 2016.

[16] Krause, T., and Ostermann, J.: Damage detection for wind turbine rotor blades using airborne sound, Structural Control Health Monitoring, Vol.27 (5), pp.1-15, 2020.

[17] Maynard, K., and Trethewey, M.: Blade and Shaft Crack Detection Using Torsional Vibration Measurements Part 1: Feasibility Studies, Noise & Vibration Worldwide, Vol.31, pp.9-15, 2020.

[18] Jinghui, X., Baijie, Q., Meiru, L., Zhibo Y., and Xuefeng, C.: Crack propagation monitoring of rotor blades using synchro extracting transform, Journal of Sound and Vibration, Vol. 509, 116253, pp.1-17, 2021.

[19] Ogbonnaya, E., Poku, R., Ugwu, H., Johnson, K., Orji, J. and Samson, N. N.: Analysis of Gas Turbine Blade Vibration Due to Random Excitation, Gas Turbines - Materials, Modeling and Performance. London, United Kingdom: Intech-Open, 2015.

[20] Santos, F., Peeters, B., Van der Auweraer., H., Góes, L.C.S., and Desmet, W.: Vibration-based damage detection for a composite helicopter main rotor blade, Case Studies in Mechanical Systems and Signal Processing, Vol. 3, pp. 22-27, 2016.

[21] Zhenfang, F., Hongkun, L., Jiannan, D., Xinwei, Z., Daitong, W., and Qiang, Z.: Blade Vibration Difference-Based Identification of Blade Vibration Parameters: A Novel Blade Tip Timing Method, Journal of Sound and Vibration, Vo.512, 116402, pp.1-19, 2021.

[22] Wensheng, Z., Yanhui, L., Meixin, X., Pengfei, W., and Jiang, J.: Vibration analysis for failure detection in low pressure steam turbine blades in nuclear power plant, Engineering Failure Analysis, Vol.84, pp.11-24, 2018.

[23] Yanfeng, W., Ming, L., and Jiawei, X.: Damage detection method for wind turbine blades based on dynamics analysis and mode shape difference curvature information, Mechanical Systems and Signal Processing, Vol.48(1–2), pp. 351-367, 2014.

[24] Aral, S., Zhu, M., Christopher, N., and Peyman, P.: Vibration-based damage detection in wind turbine blades using Phase-based Motion Estimation and motion magnification, Journal of Sound and Vibration, Vol. 421, pp.300-318, 2018.

[25] Tao, Z., Feiyun, X., and Minping, J.: A centrifugal fan blade damage identification method based on the multi-level fusion of vibro-acoustic signals and CNN, Measurement, Vol. 199, 111475, pp.1-12, 2022.

[26] Djidrov, M., Gavriloski, V. and Jovanova, J.: Vibration analysis of cantilever beam for damage detection, FME Transaction, Vol.42 (8), pp.311-316, 2014.

[27] Khazem, E., Abdullah, O., and Sabri, L.: Steady-state and vibration analysis of a WindPACT 1.5-MW turbine blade. FME Transactions, Vol.47, pp. 195-201, 2019.

[28] Qing-Ming, T.: Dimensional Analysis With Case Studies in Mechanics, Springer-Verlag, Berlin, Heidelberg Ltd., 2011.

[29] Thomas, S.: Applied Dimensional Analysis and Modeling, Elsevier Inc., Publication, 163-228, 2007.

[30] John, O. R., Sastry, G. P., David, A. D.: Applied Regression Analysis-A Research Tool, Springer-Verlag New York, Inc., Publication, 1998.

[31] Thomas, P. R.: Modern Experimental Design, John Wiley & Sons, Inc., Publication, 2007.

[32] Raymond, H. M., Douglas, C. M., and Christine, M. A.C.: Response surface methodology, John Wiley & Sons, Inc., Publication, 2009.

[33] Wowk, V.: Machinery vibrations: Measurement and Analysis, McGraw-Hill, Inc., Publication, 1991.

[34] Nakandhrakumar, R. S., Dinakaran, D., Pikton, D., and Patabiraman, J.: Mathematical models of flank wear using vibration amplitude ratio in drilling, FME Transactions, Vol. 47, pp.430-436, 2019.

NOMENCLATURE

r_1	Internal radius of the disk, mm
r_2	The external radius of the disk, mm
r_s	The radius of shaft, mm
L_S	Length of shaft
E	Young's modulus, N/mm^2

P Density, Kg/m^3
Δ Defect size, mm
N Shaft speed, rpm
W Radial load, N
f_s Shaft Frequency, Hz
f_{br} Roller defect frequency, Hz
t_b Thickness of the blade, mm
t_d Thickness of the blade, mm

Abbreviations

AE	Acoustic Emission
ANOVA	Analysis of Variation
BBD	Box–Behnken design
BHM	Blade Health Monitoring
BTT	Blade Tip Timing
CBM	Condition-based Maintenance
COMAC	coordinate modal assurance criterion
DOE	Design of Experiments
FEM	Finite Element Modelling
FOD	foreign object damage
IR	Infra-Red
MSDC	Mode Shape Difference Curvature
NHFA	Non-Harmonic Fourier Analysis
NDE	Non-Destructive Evaluation
PC	Principal component
SHM	Structural Health Monitoring

ЕМПИРИЈСКИ МОДЕЛ КОЈИ ИНТЕГРИШЕ ДИМЕНЗИОНУ АНАЛИЗУ И БОК-БЕХНКЕН ДИЗАЈН ЗА ДЕТЕКЦИЈУ ПУКОТИНА У ЛОПАТИЦАМА ВЕНТИЛАТОРА РОТОРА

И.М. Џамадар, А.К. Патил, П.К. Самал, Б. Суреша

Због континуираног рада и грешака у производњи, пукотине од замора могу се појавити након радног времена; ово узрокује квар лопатице вентилатора и потенцијално уништава цео мотор, турбо машинерију или ротирајуће машине сличне врсте. Овај рад се фокусира на праћење стања лопатица вентилатора за откривање пукотина које се јављају у овим лопатицама анализом одзива на вибрације. Математичка формулација се врши коришћењем матричне методе димензионалне анализе, која зависи од основних величина система јединица силе, дужине, времена и температуре (ФЛТΘ). Нумеричка анализа у АНСИС софтверу је урађена да би се схватио хармонијски одговор оштрице за стање напукнуте оштрице. Експериментисање се такође спроводи на машинској опреми за симулацију квара Тиера, где се мере и анализирају одзиви на вибрације ради откривања пукотина у лопатицама. Испитивања су изведена за три различите пукотине различите дужине и анализирана различитим параметрима као што је брзина оптерећења, за које су планирани експерименти применом Бок-Бехнкенове методе пројектовања. Резултати испитивања су потврђени развијеним једначинама модела, а уочене су значајне сличности између аналитичке, нумеричке и експерименталне анализе. Стога ће предложена студија помоћи да се открију пукотине на лопатицама, чиме ће се смањити озбиљне незгоде или квар машине.